JMES The International Journal of
Mechanical Engineering and Sciences
https://iptek.its.ac.id/index.php/jmes
e-ISSN 2580-7471

Analysis of the Electromagnetic Vibration Absorber (EMVA) Mechanism Placement in the MDoF System towards Vibration Reduction and Generated Electrical Energy

Wiwiek Hendrowati[1*], Aida Annisa Amin Daman[1], Harus Laksana Guntur[1], Nugraha Merdekawan[2]

[1]Department of Mechanical Engineering, Institut Teknologi Sepuluh Nopember, Surabaya 60111, Indonesia
[2]Master Program Students, Department of Mechanical Engineering, ITS, Surabaya 60111, Indonesia

Received: 6 January 2023, Revised: 25 March 2023, Accepted: 27 March 2023

Abstract

This research was conducted to determine the effect of the Electromagnetic Vibration Absorber (EMVA) placement position to reduce the main system's vibration and generate energy. This study reported the simulation and experimental results on the main system, which was excited by an external force, and the resulting vibration was reduced with an EMVA. The model of the main system and the EMVA were on a laboratory scale. The main system consisted of a steel plate as a main mass that was supported by four springs. The main system was subjected to an excitation force from the DC motor. The results show that both the simulation approach and experiment correspond well with each other. The reduction of the main system's vibration was found to be affected by the position of EMVA. The maximum vibration reduction in translation, rolling, and pitching directions occurred at different positions, which were at point 7 for translation direction, and at point 1 for rolling and pitching directions. Meanwhile, the highest power generation occurred when the EMVA was placed at point 1.

Keywords: Electromagnetic, electromagnetic vibration absorber, vibration reduction

1. Introduction

Vibration, a natural occurrence, is one type of response of a mechanical system that is either caused by excitation forces or changes in operating conditions as a function of time [1]. However, if the vibration occurs excessively, it can cause defects and shorten the life of a machine [2]. One way to reduce vibration rate is using Dynamic Vibration Absorber (DVA). The purpose of installing DVA is to absorb excessive kinetic energy and change the natural frequency of a system. This idea was pioneered by Frahm in 1909 [3]. In the reduction process that occurs in DVA, the excess vibrations are absorbed by the absorber mass and the absorber spring. The modification of DVA has been studied to reduce the vibration of various systems. The use of an inerter in DVA to reduce the natural frequency of a system was conducted by Chen et al. [4]. This inerter-DVA was also used by Hu and Chen [5] in their study and resulted in a widened frequency band. Shen et al. [6] applied the inerter-DVA in vehicle suspension, and the result showed that the inerter-DVA effectively reduced the acceleration of the body and the deflection of the suspension. Meanwhile, non-linear damping was added to the DVA system to reduce the linear structure's vibration [7]. The DVA was later modified to reduce the vibration in the rotational motion by using mass and spring in the radial direction of a shaft called the Radial Vibration Damper (RVD) [8]. However, the dissipated energy from vibration reduction can be utilized to provide potential energy.

Rapid technology development makes it easy to figure out how to convert waste energy into potential electrical energy, called energy harvesting. The theory of delayed resonator is used in vibration absorbers to enhance energy harvesting [9]. The application of a transmission box is used to transfer the motion of ocean waves into the motion of the generator, which provides electrical energy [10]. However, there are still some mechanical losses in the transmission box. Therefore, piezoelectric is utilized to effectively reduce vibration and harvest energy [11–13]. Piezoelectric consists of a crystal that is placed between two metal plates. When mechanical pressure is applied to the metal plate, it forces the electric charges in the crystal collected by the metal plate and produces voltage. Its small design can be a positive value. However, it can only produce a small amount of electricity. Various things may affect the efficiency and voltage output, as discovered by previous researchers [14–19]. One research study by Ahmed et al. [20] was conducted to investigate ways to harvest energy from vibration. They studied electromag-

*Corresponding author. Email: wiwiek@me.its.ac.id.

netic vibration energy harvesting with free/impact motion using the DVA mechanism with a mass made from the magnet that can move freely within a certain distance. Sometimes it hit the frame, and sometimes it did not, depending on the excitation. Outside the frame, there were coil springs to convert fluctuating magnetic fields into electricity. This mechanism was designed for low-frequency operations. Rahman et al. [21] further modeled and optimized an electromagnetic energy harvesting device, with the absorber mass moving the magnet relative to a coil to transform mechanical energy into electrical energy.

In this study, vibration in the main system is designed to represent vibration in machines with three natural frequencies (48.85 rad/s, 67.38 rad/s, and 70.05 rad/s) using a vibration simulator. The EMVA mechanism is designed to generate electricity by utilizing coil springs, a magnet, and coil wire. This study aims to determine the acceleration response vibrations with the directions of translation, rolling, and pitching, as well as the electrical energy generated at several placements to get the optimum position to use the EMVA.

2. Research Method

The electromagnetic vibration absorber had two main components, namely mechanical and electrical components. Mechanical components included a neodymium magnet and steel coil spring. The absorber mass was tuned with a ratio of 1:20 of the main system mass to get the optimum vibration reduction [1]. Adding the DVA gave the system a new natural frequency. The DVA mass to main system mass ratio affected the new natural frequency range. The DVA mass, which had a value of 1/20 to the mass of the absorber, made the main system have the smallest amplitude at the fundamental natural frequency. At that frequency, the DVA mass could dampen vibrations optimally. Meanwhile, the absorber's stiffness designed for the EMVA had the same value of natural frequency as the fundamental natural frequency of the main system. An experimental stiffness test was then carried out by measuring the spring deflection with an overloading neodymium magnet. Then, the stiffness was calculated using Hooke's Law as written in Equation (1).

$$k = \frac{F}{\Delta x} \tag{1}$$

The electrical component involved coil wire wrapped around the case connected with the oscilloscope. Two sources of damping force in EMVA came from mechanical friction and electromagnetic induction. To get the mechanical damping coefficient, an impact test was carried out. Spring and mass absorber, which was connected to the accelerometer, was given an initial force to get the logarithmic decrement response. Figure 1 shows the logarithmic decrement response in the time domain. Then, the mechanical damping coefficient was calculated using Equation (2).

$$c = 2m\sqrt{\frac{k}{m}} \times \left(\frac{\ln\left(\frac{x_1}{x_{n+1}}\right)}{2\pi} \right) \tag{2}$$

The electrical damping coefficient was obtained using Lorentz's and Lenz's Law as written in Equation (3).

$$c = \frac{B_r t_m \delta}{\mu_r} \ln\left(\frac{t_m + \mu_r p_m}{t_m + \mu_r (x - l_1)} \cdot \frac{t_m + \mu_r (l_2 - x)}{t_m} \right) \tag{3}$$

where:

$$\delta = \frac{\epsilon A Z}{\mu_r \rho l_w d_w^2} \pi \left(di + \frac{(1+Z)}{2} dw \right) \cdot \left(\frac{1}{(t_m + \mu_r (x - l_1))} - \frac{1}{t_m + \mu_r p_m} + \frac{1}{t_m + \mu_r (l_2 - x)} - \frac{1}{t_m} \right)$$

$$\epsilon = \frac{\pi}{4} \left(Z d_i^2 + (Z + Z^2) d_i d_w + \frac{Z(Z+1)(2Z+1)}{6} d_w^2 \right) \mu_r B_r t_m$$

$$x = (x_1 + a\alpha + b\beta - x_2)$$

with :

c	:	Damping coefficient (Ns/m)
m	:	Mass (kg)
k	:	Stiffness (N/m)
x_1	:	Average of first amplitude and its nearby
x_{n+1}	:	Average of n+1 amplitude and its nearby
B_r	:	Magnetic field (T)
t_m	:	Magnetic diameter (m)
p_m	:	Magnetic bar length (m)
μ_r	:	Relative permeability of air
x	:	Absorber translational displacement (m)
l_w	:	Coil wire length (m)
Z	:	Number of piles of coils

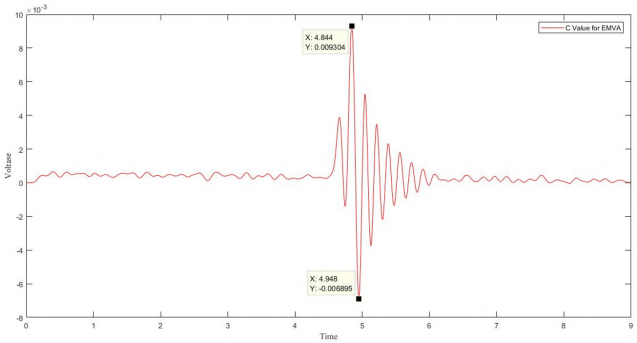

Figure 1. Logarithmic decrement response in the time domain.

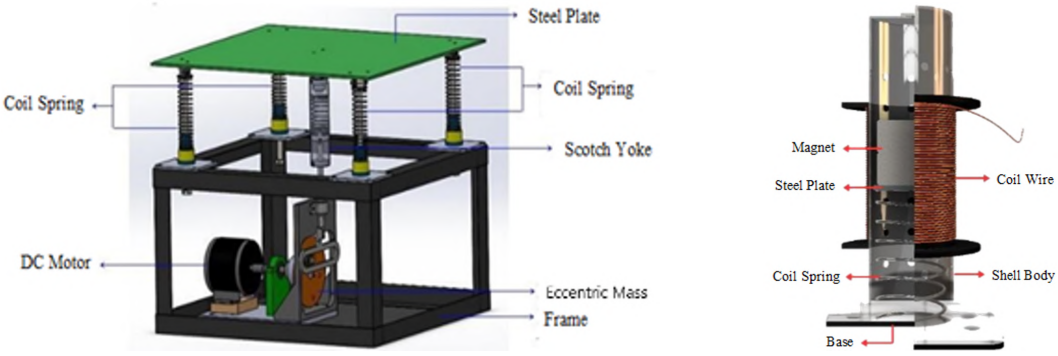

(a) Main system. **(b)** EMVA.

Figure 2. Analysis model.

The main system was a steel plate supported by four springs with different stiffness and damping constants. The excitation force was from the DC motor connected to a scotch yoke, so the main system got a sinusoidal excitation force as an input. The main system was designed to represent vibration in a machine with three natural frequencies. The analysis model of the main system and EMVA are shown in Figure 2. The main system parameters were also tested using the above method. In this research, a simulation and experimental method were carried out in response to the accelerated vibrations with the directions of translation, rolling, and pitching, as well as the electrical energy generated by the EMVA mechanism. This research determined the impact of EMVA placement and optimum position on the main system.

3. Theoretical Background and Mathematical Model

In order to perform the simulation analysis, motion equations were needed to convert a state variable into a simulation block diagram. From the simulation block diagram, the prediction of vibration responses and energy generation before and after using EMVA was simulated in MATLAB Simulink software.

3.1. Equation of Motion For The Main System Without EMVA

Figure 3 shows the free body diagram of the main system without EMVA. The displacement in the main system followed the translational, rolling, and pitching directions due to differences in the stiffness and damping constants of the mass support spring of the main system. The main system motion without EMVA in the translational, rolling, and pitching direction are described by Equation (4), (5), and (6), respectively.

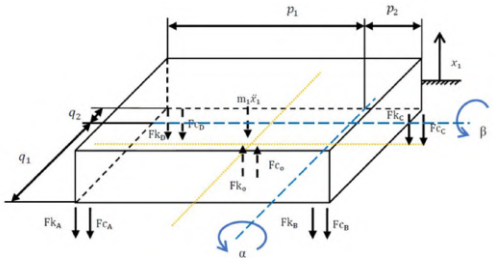

(a) Translational direction.

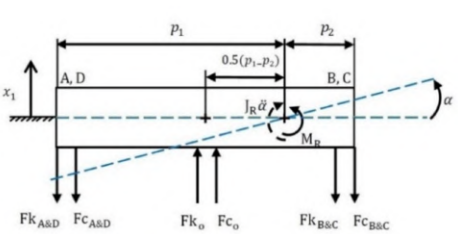

(b) Rolling direction.

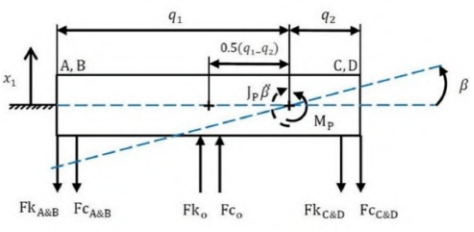

(c) Pitching direction.

Figure 3. Free body diagram of the main system without EMVA.

$$+\uparrow \sum F_{x1} = m_1 \ddot{x}_1$$
$$F_{KO} + F_{CO} - F_{KA} - F_{CA} - F_{KB} - F_{CB} - F_{KC} - F_{CC} - F_{KD} - F_{CD} = m_1 \ddot{x}_1 \quad (4)$$

$$\oplus \sum M_R = J_R \ddot{\alpha}$$
$$-F_{KO}[0.5(p_1 - p_2)] - F_{CO}[0.5(p_1 - p_2)] + F_{KA}p_1 + F_{CA}p_1 - F_{KB}p_2 - F_{CB}p_2 - F_{KC}p_2 - F_{CC}p_2 + F_{KD}p_1 + F_{CD}p_1 = J_R \ddot{\alpha} \quad (5)$$

$$\oplus \sum M_P = J_P \ddot{\beta}$$
$$-F_{KO}[0.5(q_1 - q_2)] - F_{CO}[0.5(q_1 - q_2)] + F_{KA}q_1 + F_{CA}q_1 + F_{KB}q_1 + F_{CB}q_1 - F_{KC}q_2 - F_{CC}q_2 - F_{KD}q_2 - F_{CD}q_2 = J_P \ddot{\beta} \quad (6)$$

3.2. Equation of Motion For The Main System With EMVA

Figure 4 shows a free body diagram of the main system with an EMVA and the EMVA itself. It appeared that the mass of the main system was affected m_2, F_{k2}, and F_{c2}. The main system motion with EMVA in the translational, rolling, pitching direction, and the EMVA itself are described by Equation (7), (8), (9), and (10), respectively.

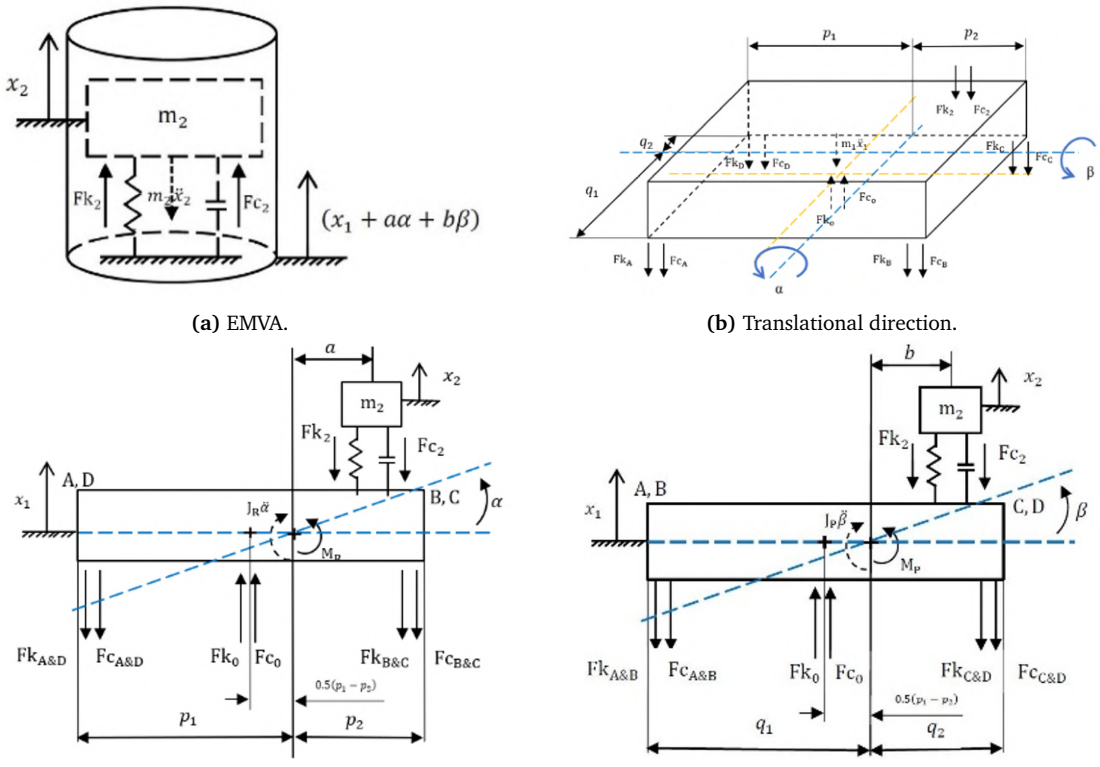

(a) EMVA.

(b) Translational direction.

(c) Rolling direction.

(d) Pitching direction.

Figure 4. The dynamic model of the main system motion with EMVA.

$$+\uparrow \sum F_{x1} = m_1 \ddot{x}_1$$
$$F_{KO} + F_{CO} - F_{KA} - F_{CA} - F_{KB} - F_{CB} - F_{KC} - F_{CC} - F_{KD} - F_{CD} - F_{K2} - F_{C2} = m_1 \ddot{x}_1 \quad (7)$$

$$\begin{gathered}\circlearrowleft+\sum M_R = J_R\ddot{\alpha} \\ F_{KA}p_1 + F_{CA}p_1 - F_{CB}p_2 - F_{CC}p_2 + F_{KD}p_1 + F_{CD}p_1 - \\ F_{KO}[0.5(p_1 - p_2)] - F_{CO}[0.5(p_1 - p_2)] - F_{K2}a - F_{C2}a - F_{KC}p_2 = J_R\ddot{\alpha}\end{gathered} \tag{8}$$

$$\begin{gathered}\circlearrowleft+\sum M_P = J_P\ddot{\beta} \\ F_{KA}q_1 + F_{CA}q_1 + F_{KB}q_1 + F_{CB}q_1 - F_{KC}q_2 - F_{CC}q_2 - F_{KD}q_2 - \\ F_{CD}q_2 - F_{KO}[0.5(q_1 - q_2)] - F_{CO}[0.5(q_1 - q_2)] - F_{K2}b - F_{C2}b = J_P\ddot{\beta}\end{gathered} \tag{9}$$

$$\begin{gathered}+\uparrow\sum F_{x2} = m_2\ddot{x}_2 \\ F_{K2} + F_{C2} = m_2\ddot{x}_1 \\ m_2\ddot{x}_2 - k_2x_1 - k_2a\alpha - k_2b\beta - c_2\dot{x}_1 + c_2\dot{x}_2 - c_2a\dot{\alpha} - c_2b\dot{\beta} = 0\end{gathered} \tag{10}$$

with :

m_1 : The mass of main system (kg)
k_0 : Excitation spring stiffness constant (N/m)
k_i : Spring stiffness constant of m_1 at point i(N/m)
c_0 : Exciter spring damping constant (Ns/m)
c_i : Damping constant of m_1 at point i (Ns/m)
x_0 : Excitation spring displacement (m)
x_i : Main system mass displacement (m)

3.3. Equation of The Electrical System

Figure 5 shows an electrical circuit diagram of EMVA. EMVA generated electrical energy when the absorber mass oscillated vertically in the copper coil. Electrical energy consisted of a voltage generator and electric power. The EMVA electrical voltage generation described by Equation (11).

$$e_{total} = \frac{\epsilon}{d_w\mu_r}\dot{x}\left(-\frac{1}{t_m + \mu_r p_m} + \frac{1}{t_m + \mu_r(x - l_1)} + \frac{1}{t_m + \mu_r(l_2 - x)} - \frac{1}{t_m}\right) \tag{11}$$

$$\dot{x} = (\dot{x_1} + a\dot{\alpha} + b\dot{\beta} - \dot{x_2})$$

Whereas for EMVA electrical power can be calculated using Equation (12).

$$P = \frac{e_{total}^2}{R} \tag{12}$$

with :

m_2 : The mass of EMVA (kg)
k_2 : EMVA spring stiffness constant (N/m)
c_2 : EMVA spring damping constant (Ns/m)
x_2 : EMVA displacement (m)
I : A, B, C, or D
R : External resistance (Ω)
L : Length of coil (m)
D_1 : Diameter of coil (m)
$e_i(t)$: Induced EMF(V)
i : Electric current (A)
X_2 : Magnetic displacement (m)
$\dot{x}$: Magnetic speed (m/s)
x : Absorber translational displacement (m)

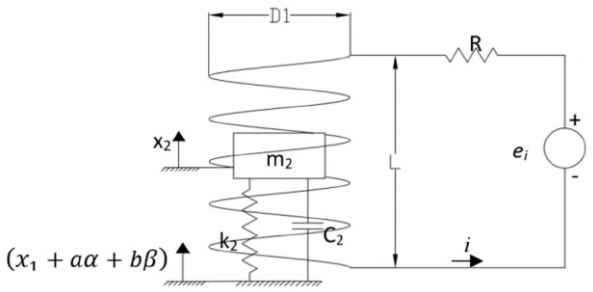

Figure 5. Schematic of the electrical system in EMVA.

3.4. Simulation Parameter

The parameters used in this study are shown in Table 1. Parameter values were obtained from measurement or testing tools that have undergone manufacturing.

3.5. Research Variations

The research was carried out with ten EMVA position variations in the main system. The scheme of EMVA placement position variation is shown in Figure 6. Point 7 was the centroid of the system. The EMVA was placed at one point at a time. Then, the vibration responses of the main system were collected.

4. Experiment

An experiment was conducted to validate the governed mathematical model, as shown in Figure 7. An accelerometer sensor connected with an oscilloscope was used to obtain the translational, rolling, and pitching dynamic responses and the output power of EMVA. Periodical

Table 1. Main system parameters and EMVA.

Parameter	Symbol	Value	Unit
Main system mass	m_1	5.4	kg
Main system moment of inertia	J_R, J_P	0.1125	$kg \cdot m^2$
Spring A stiffness constant	k_A	1840.3813	N/m
Spring B stiffness constant	k_B	3680.7627	N/m
Spring C stiffness constant	k_C	5521.1439	N/m
Spring D stiffness constant	k_D	2760.572	N/m
Spring A damping constant	c_A	8.3429	Ns/m
Spring B damping constant	c_B	26.9344	Ns/m
Spring C damping constant	c_C	41.3986	Ns/m
Spring D damping constant	c_D	23.3259	Ns/m
EMVA mass	m_2	0.3845	kg
Magnet diameter	t_m	0.039	m
Magnetic field direction	B_r	1.2	T
Magnet thickness	p_m	0.038	m
Length of coil	l_k	0.08	m
Diameter of coil wire	d_w	0.25	mm
Coil type resistance	ρ	1.68×10^{-8}	Ωm
Number of coil piles	$Z.N$	2600	$coil$
Air permeability	μ_r	1.05	
Spring stiffness constant	k_D	581.1731	N/m
Spring damping constant	c_A	2.1924	Ns/m
External Resistance	R	100	Ω

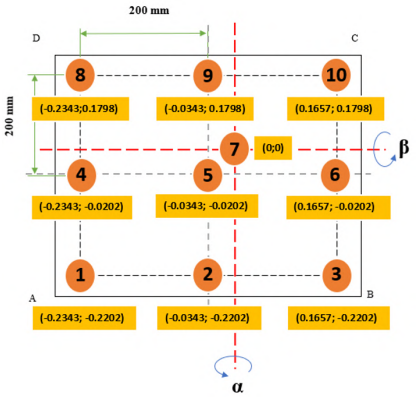

Figure 6. Ten EMVA placement positions in the main system.

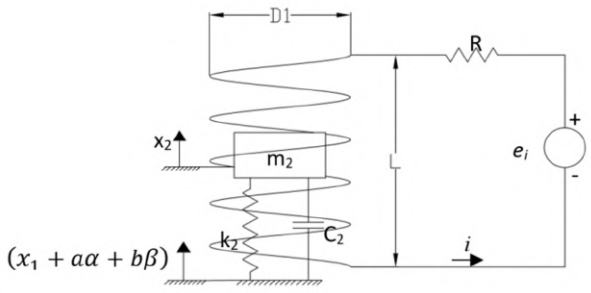

Figure 7. Experimental set up.

input with a frequency of 48.85 rad/s was applied to the bottom of the main system, representing the machine's operating condition. The dynamic responses and generated electricity from EMVA were measured, analyzed, and discussed.

5. Results, Analysis, and Discussion

5.1. Dynamic Responses of Main System without and with EMVA simulation approach

The excitation force from the DC motor was transmitted to the scotch yoke, so the input was a sinusoidal wave with a frequency of 48.85 rad/s. After simulating the block diagram by entering the parameter values in Table 1, the data of the main system with and without EMVA acceleration response in translational, rolling, and pitching directions were obtained. Figure 8 shows the simulated acceleration responses of the main system in a rolling direction at point 7.

From the simulation, the RMS acceleration response of the rolling direction had the highest value. This was because the spring's constant equivalent of the rolling motion direction was smaller than the pitching direction, which resulted in the rolling displacement angle being greater than the pitching displacement angle. Therefore, the vibration deviation in the rolling direction was greater than in the pitching direction. Based on the value of RMS, the acceleration response of translational, rolling, and pitching direction of the main system with EMVA had mostly a lower value of RMS rather than the RMS of the main system without EMVA. RMS_1 stands for the acceleration response of the main system without EMVA, and RMS_2 stands for the acceleration response of the main system with EMVA. The vibration reduction could then be expressed as shown in Equation (13).

$$vibration\ reduction = \frac{RMS_1 - RMS_2}{RMS_1} \cdot 100\% \quad (13)$$

The vibration reduction for each placement variation in translation, rolling, and pitching direction was then stated as a surface contour, as shown in Figure 9.

The reduction of vibration acceleration response of the main system in the translational direction is shown in Figure 9(a). From the surface contour above, the reduction in vibration in the translational direction decreased as the distance of EMVA to the main system's rotary axis increased. This statement was proved by acceleration response reduction in translational direction simulation at

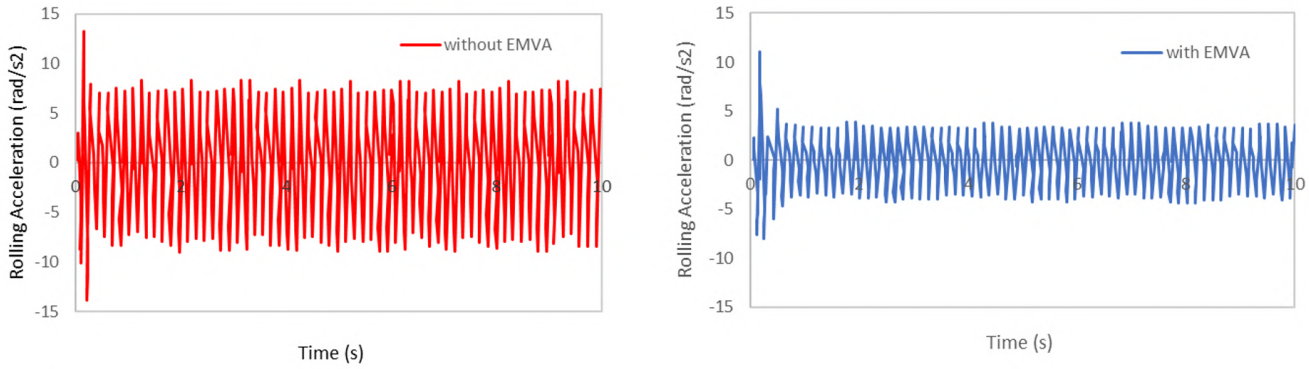

Figure 8. Simulated acceleration responses of the main system in rolling direction position with EMVA positions at point 7.

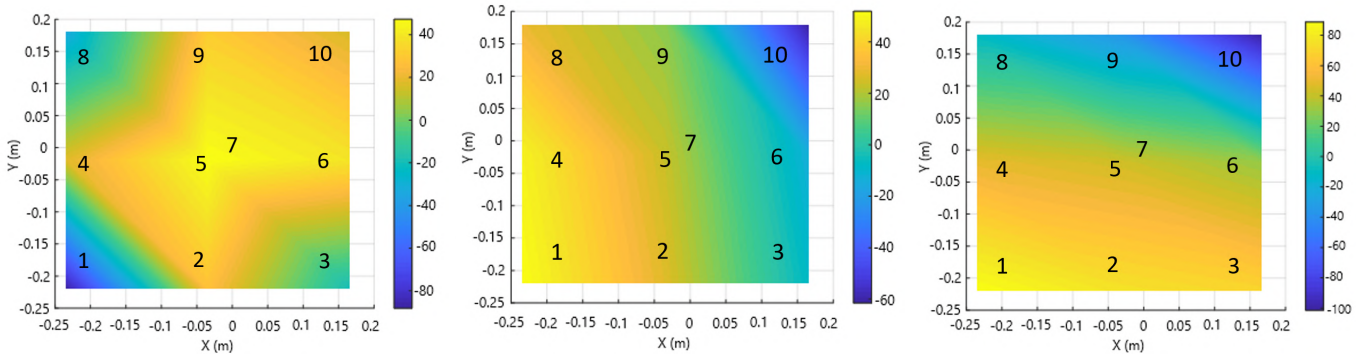

(a) Translational direction. **(b)** Rolling direction. **(c)** Pitching direction.

Figure 9. Surface contour of simulated vibration reduction of the main system after placing EMVA at several position variations.

point 1 with the lowest value of -88.11%. Point 7 had the highest acceleration response reduction with a value of 50.52%. The distance of point one was 0.3215 m from the center of the rotary axis. Point 1 was where the EMVA was placed the farthest from the center of the rotary axis, so placing EMVA at point 1 did not reduce the acceleration response of vibrations in the translational direction. Furthermore, point 7 was where the rotary axis was located, so there was the largest acceleration response decrease in the translational direction. The cause of the reduced acceleration response of the translational direction vibrations when approaching the excitation source was due to the base motion being big enough in the EMVA system, and the vibration from the base motion was countered by force from the mass, the stiffness force, and the damping force of the EMVA system.

Besides affecting the response of translational vibrations, the placement of EMVA also affected the acceleration response of rolling and pitching vibrations. From Figure 9(b) and 9(c), the reduction of vibration response in the rolling and pitching directions increased as the EMVA distance toward the rotary axis of each vibration direction increased. The most significant reduction in acceleration response of rolling and pitching directions was at point 1, with a value of 51.86% and 86.78%, respectively. Meanwhile, the smallest reduction in acceleration response of rolling and pitching directions was at point 10, with a value of -61.43% and -101.32%, respectively. Point 10 was the point where the mass support spring of the main system had the highest stiffness value, while point 1 was the lowest. At point 10, where the spring with the biggest stiffness constant was located, the vibration acceleration response of the rolling and pitching directions with the EMVA exceeded the acceleration response of the main system without EMVA. In other words, EMVA did not reduce vibration but provided an extra excitation force to the main system.

5.2. Experimental Dynamic Responses of The Main System with and without EMVA

In this study, an experimental method was also carried out to validate the corresponding mathematical model based on simulation. Similar to the simulation, the analysis was performed experimentally to determine the reduction of vibrations in the main system and the energy generation in the form of electrical energy generated by the system absorber (EMVA). The desired vibration response in this experiment was the same as the simulation approach, which was the acceleration responses in translation, rolling, and pitching directions. A vibration response reader was necessary to find out the vibration response of the main system, namely an oscilloscope. However, the results of the vibration response read on the oscilloscope were time and voltage data. Thus, the data must be converted into an acceleration response for vibrational responses in translational, rolling, and pitching directions. Furthermore, after converting the data from the oscilloscope, the data was filtered and smoothed using MATLAB Simulink to eliminate noise during the test. The experimental acceleration responses of the main system in translation direction with EMVA positions at point 7 can be seen in Figure 10.

As before, the vibration reduction for each placement variation in translation, rolling, and pitching directions were calculated and stated as a surface contour, as shown in Figure 11.

Both the simulated and experimental surface contours had a similar vibration reduction area in translational, rolling, and pitching directions. The reduction of experimental acceleration response toward translation direction at point 1 had the lowest value of -68.6%. Whereas point 7 had the highest value of 62.61%. The greatest reduction in the acceleration response of rolling and pitching was at point 1, with a value of 59.49% and 91.9%, respectively. In contrast, the smallest reduction in the

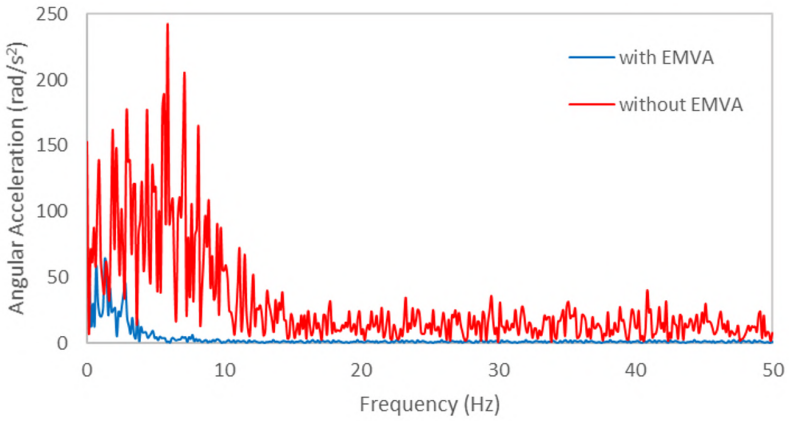

Figure 10. Experimental acceleration responses of the main system in translation direction with EMVA positions at point 7.

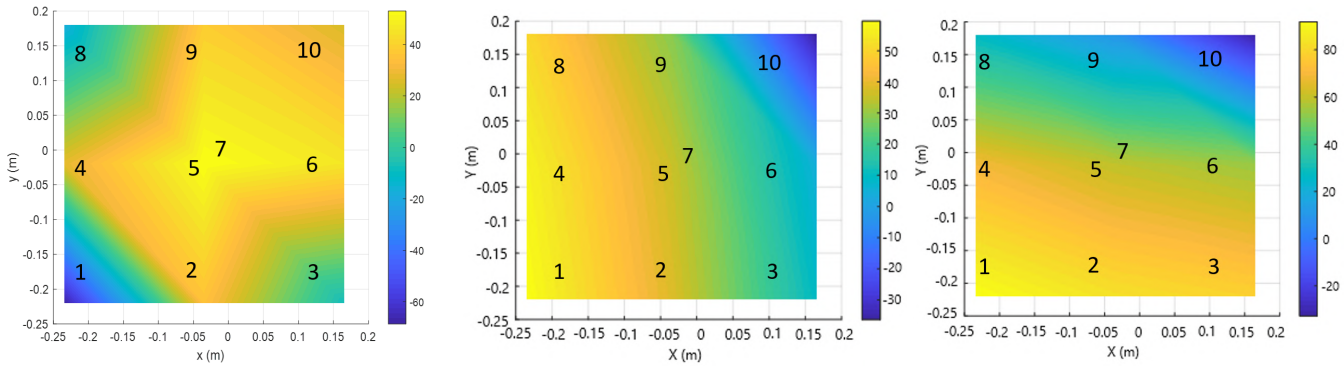

(a) Translational direction. **(b)** Rolling direction. **(c)** Pitching direction.

Figure 11. Surface contour of experimental vibration reduction of the main system after placing EMVA at several position variations.

acceleration response of rolling and pitching was at point 10, with a value of -36.34% and -32.78%, respectively. A statistically independent T-Test method was used to add correction value in the simulated data to ensure that the simulation approach and experiment did not have a significantly different value. With a confidence level of 95%, simulated and experimental data did not have different significant values.

5.3. Electrical Energy Generation

Electrical energy was generated using the electromagnetic principle, where the magnet in the EMVA oscillated and created a magnetic field, cutting perpendicular to the coil of the EMVA, resulting in electromagnetic induction. The simulated power generation was done by using MATLAB Simulink by entering parameter values in Table 1. Meanwhile, the power generation experiment data was obtained from an oscilloscope after smoothing and filtering, as shown in Figure 12.

The power generated in each position variation was then stated as surface contour, as shown in Figure 13. The surface contours show that the response of electric energy generation was increased when EMVA was placed at the point where the vibration deviation increased. This statement was backed by the value of the largest electrical energy generation response when EMVA was placed at point 1 with a value of 2.7975×10^{-5} Watt for the simulation and 3.62×10^{-9} Watt for the experiment. In contrast, the smallest generation of electrical energy occurred when EMVA was placed at point 5, with a value of 2.6775×10^{-6} Watt for the simulation and 1.81×10^{-5} Watt for the experiment. This phenomenon was caused by the main mass supported by a spring with the smallest stiffness constant at point 1, so the main mass had the largest deviation for the translational direction at point 1. In contrast, point 5 was where the main mass had the smallest deviation toward the translational direction, resulting in the energy generated at position 5 having the smallest value. It could be concluded that the generated energy was optimal when the EMVA was placed at point 1.

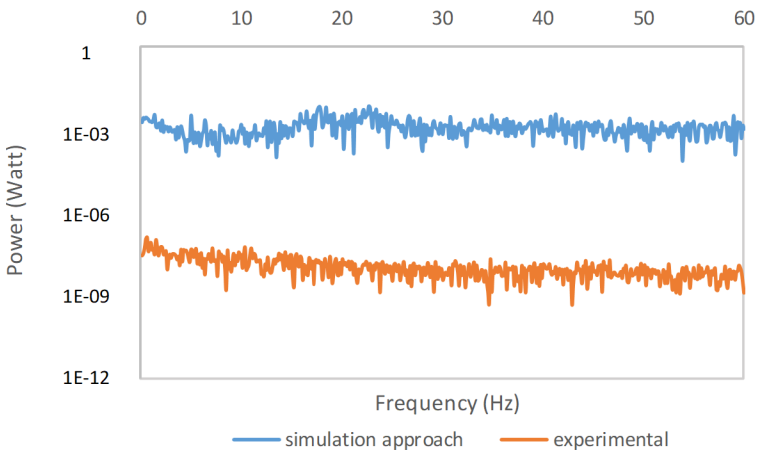

Figure 12. Power generation of EMVA placement at point 1.

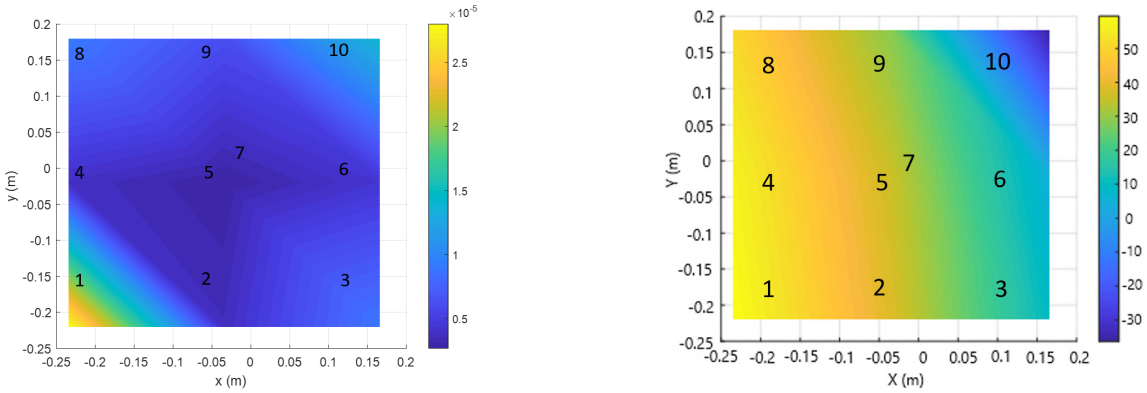

(a) Simulation.

(b) Experimental.

Figure 13. Surface contour of EMVA power generation.

6. Conclusion

The electromagnetic vibration absorber (EMVA) dynamic responses and output power generation have been reported. The designed main system with and without EMVA was mathematically modeled and simulated. The simulated vibration reduction and energy generation were compared to experimental vibration reduction and energy generation. All graphs show that the simulation and experimental methods have the same trendline. However, the simulation result values were higher than the experiments. In the translational direction, vibration reduction increased as the EMVA was closer to the rotating axis. The highest vibration reduction was at point 7 with a 62.61% reduction, while the lowest was at point 1 with a -68.6% reduction. The reduction of vibration response in the rolling and pitching directions increased as the EMVA distance toward the rotary axis of each vibration direction increased. The highest reduction for rolling and pitching directions was at point 1, which were 59.49% and 91.9%, respectively. In contrast, the lowest reduction for rolling and pitching directions was at point 10, which were -61.43% and -101.32%, respectively. The energy generation was higher as the vibration deviation of the main system increased, which occurred when EMVA was placed at point 1 with 3.62×10^{-9} Watt energy generated.

References

[1] S. S. Rao, *Mechanical Vibrations, 5th Eddition*. NJ 07458, Pearson Education, Inc, 2010.

[2] W. Hendrowati, H. L. Guntur, and M. Solichin, "Optimizing the value of reduction and generating energy on mechanism of cantilever piezoelectric vibration absorber (cpva)," vol. 1983, p. 030015, 2018.

[3] H. Frahm, "Device for damping vibrations of bodies.," 1911. US Patent 989958.

[4] M. Z. Chen, Y. Hu, L. Huang, and G. Chen, "Influence of inerter on natural frequencies of vibration systems," *Journal of Sound and Vibration*, vol. 333, no. 7, pp. 1874–1887, 2014.

[5] Y. Hu and M. Z. Chen, "Performance evaluation for inerter-based dynamic vibration absorbers," *International Journal of Mechanical Sciences*, vol. 99, pp. 297–307, 2015.

[6] Y. Shen, L. Chen, X. Yang, D. Shi, and J. Yang, "Improved design of dynamic vibration absorber by using the inerter and its application in vehicle suspension," *Journal of Sound and Vibration*, vol. 361, pp. 148–158, 2016.

[7] J. Love and M. Tait, "Estimating the added effective damping of sdof systems incorporating multiple dynamic vibration absorbers with nonlinear damping," *Engineering Structures*, vol. 130, pp. 154–161, 2017.

[8] W. Hendrowati, H. L. Guntur, A. A. A. Daman, and D. Anggitasari, "Radial vibration damper (rvd) mechanism validation for long thin shaft at lathe machine," *AIP Conference Proceedings*, vol. 2187, no. 1, p. 050025, 2019.

[9] A. S. Kammer and N. Olgac, "Delayed-feedback vibration absorbers to enhance energy harvesting," *Journal of Sound and Vibration*, vol. 363, pp. 54–67, 2016.

[10] A. A. A. Daman, W. Hendrowati, and H. L. Guntur, "Analysis of a single vertical pendulum mechanism on the pontoon-boat as a wave energy harvester," *The International Journal of Mechanical Engineering and Sciences*, vol. 2, no. 2, pp. 1–9, 2018.

[11] C. Madhav and S. F. Ali, "Harvesting energy from vibration absorber under random excitations," *IFAC-PapersOnLine*, vol. 49, no. 1, pp. 807–812, 2016. 4th IFAC Conference on Advances in Control and Optimization of Dynamical Systems ACODS 2016.

[12] C.-Y. Lee and J.-H. Lin, "Incorporating piezoelectric energy harvester in tunable vibration absorber for application in multi-modal vibration reduction of a platform structure," *Journal of Sound and Vibration*, vol. 389, pp. 73–88, 2017.

[13] W. Larbi and J.-F. Deü, "Reduced order finite element formulations for vibration reduction using piezoelectric shunt damping," *Applied Acoustics*, vol. 147, pp. 111–120, 2019. Special Issue on Design and Modelling of Mechanical Systems conference CMSM'2017.

[14] R. Tardiveau, F. Giraud, A. Amanci, F. Dawson, C. Giraud-Audine, M. Amberg, and B. Lemaire-Semail, "Power consideration in a piezoelectric generator," *Smart Materials Research*, vol. 2013, p. 410567, Sep 2013.

[15] A. Nechibvute, A. Chawanda, and P. Luhanga, "Finite element modeling of a piezoelectric composite beam and comparative performance study of piezoelectric materials for voltage generation," *ISRN Materials Science*, vol. 2012, p. 921361, Sep 2012.

[16] P. R. Bhaskaran, J. D. Rathnam, S. Koilmani, and K. Subramanian, "Multiresonant frequency piezoelectric energy harvesters integrated with high sensitivity piezoelectric accelerometer for bridge health monitoring applications," *Smart Materials Research*, vol. 2017, p. 6084309, Jan 2017.

[17] A. Čeponis and D. Mažeika, "Investigation of multi-frequency piezoelectric energy harvester," *Shock and Vibration*, vol. 2017, p. 8703680, Nov 2017.

[18] Z. Wang, X. Pan, Y. He, Y. Hu, H. Gu, and Y. Wang, "Piezoelectric nanowires in energy harvesting applications," *Advances in Materials Science and Engineering*, vol. 2015, p. 165631, Jun 2015.

[19] S. F. Ali and S. Adhikari, "Energy Harvesting Dynamic Vibration Absorbers," *Journal of Applied Mechanics*, vol. 80, 05 2013. 041004.

[20] A. Haroun, I. Yamada, and S. Warisawa, "Study of electromagnetic vibration energy harvesting with free/impact motion for low frequency operation," *Journal of Sound and Vibration*, vol. 349, pp. 389–402, 2015.

[21] M. F. Ab Rahman, S. L. Kok, N. M. Ali, R. A. Hamzah, and K. A. A. Aziz, "Hybrid vibration energy harvester based on piezoelectric and electromagnetic transduction mechanism," in *2013 IEEE Conference on Clean Energy and Technology (CEAT)*, pp. 243–247, 2013.